# HELIOS/DRAGON/NESTLE Codes' Simulation of the Gentilly-2 Loss of Class 4 Power Event


Hisham N. Sarsour
Independent Consultant
1114 Nottingham Circle
Cary, NC 27511
HishamSarsour@cs.com

Paul J. Turinsky
North Carolina State University
Raleigh, NC 27695-7909
turinsky@eos.ncsu.edu

Farzad Rahnema and Scott Mosher
Georgia Institute of Technology
Atlanta, GA 30332
farzad.rahnema@nre.gatech.edu and gt3522a@prism.gatech.edu

Dumitru Serghiuta
Canadian Nuclear Safety Commission
280 Slater Street, 7th Floor
Ottawa, Ontario K1P 5S9
serghiutad@cnsc-ccsn.gc.ca

Guy Marleau and Tanguy Courau
Ecole Polytechnique de Montreal
P.O. Box 6079, station Centre-ville
Montreal, Quebec H3C 3A7
guy.marleau@polymtl.ca


## Introduction

A loss of electrical power occurred at Gentilly-2 in September of 1995 while the station was operating at full power [1]. There was an unexpectedly rapid core power increase initiated by the drainage of the zone controllers and accelerated by coolant boiling. The core transient was terminated by Shutdown System No 1 (SDS1) tripping when the out-of-core ion chambers exceeded the 10%/sec high rate of power increase trip setpoint at 1.29 sec. This resulted in the station automatically shutting down within 2 sec of event initiation. In the first 2 sec, 26 of the 58 SDS1 and SDS2 in-core flux detectors reached there overpower trip (ROPT) setpoints. The peak reactor power reached approximately 110%FP.

Reference 1 presented detailed results of the simulations performed with coupled thermalhydraulics and 3D neutron kinetics codes, SOPHT-G2 and the CERBERUS module of RFSP, and the various adjustments of these codes and plant representation that were needed to obtain the neutronic response observed in 1995.

The purposes of this paper are to contrast a simulation prediction of the peak prompt core thermal power transient versus experimental estimate, and to note the impact of spatial discretization approach utilized on the prompt core thermal power transient and the channel power distribution as a function of time. In addition, adequacy of the time-step sizes employed and sensitivity to core's transient thermal-hydraulics conditions are studied. The work presented in this paper has been performed as part of a project sponsored by the Canadian Nuclear Safety Commission (CNSC). The purpose of the project was to gather information and assess the accuracy of best estimate methods using calculation methods and codes developed independently from the CANDU industry.

The simulation of the accident was completed using the NESTLE core simulator [2], employing cross sections generated by the HELIOS lattice physics code [3], and incremental cross sections generated by the DRAGON lattice physics code [4] based upon HELIOS generated cross sections. Core thermal-hydraulic conditions, zone controller levels, and control device positions as a function of time are all taken from the CERBERUS/SOPHT-G2 [1] simulation of this event. To address sensitivity to spatial discretization treatment, NESTLE core simulator predictions based upon the finite difference method (FDM), nodal expansion method (NM) without utilizing assembly discontinuity factors (ADF), and NM with utilizing ADF will be contrasted. Note that NESTLE Version 5 has the option to solve the two-group neutron diffusion equation via the nodal expansion method, employing a quartic polynomial flux expansion and quadratic transverse leakage representation in solving the 1-D transverse integrated diffusion equation.

## Simulation Results

Figure 1 shows the full core spatial XxYxZ mesh layout of 46x34x30, where 2 denotes fuel nodes, 1 denotes reflector nodes, and 0 denotes null nodes. This model has 380 channels with 12 bundles in each channel. The maximum number of channels in the x and y directions is 22. The lattice pitch is 28.575 cm and the bundle length is 49.53 cm. The notch was modeled in NESTLE; however, the radial boundary condition of non-reentrant current with an extrapolation distance was applied in the $D_2O$ reflector using a Cartesian ragged edge versus cylindrical geometry. Utilizing the HELIOS/DRAGON functionalized cross-sections, the predicted $k_{eff}$ values at the start of the transient are 0.99728, 0.99748, and 0.99624 for NESTLE FDM, NESTLE NM without ADF, and NESTLE NEM with ADF, respectively, implying differences with the known critical core state of -2.72, -2.52 and –3.76 mk.

Table I shows the time steps used for the base case. Other cases with finer time steps are based on the time steps that are in Table I. The channel relative power distribution comparison at the start of the transient as predicted by NESTLE NM with ADF and NESTLE FDM is shown for Figure 2. NESTLE NM with ADF is selected as the reference to compare the other spatial discretization treatments against since this treatment is expected to be most accurate. It is observed that the FDM rolls the channel relative power distribution from the core interior to the core edge. The causes of these prediction differences come from two sources: the finite difference truncation error and the cross section homogenization error. To isolate the effect of ADFs, Figure 3 contrasts the channel relative power distribution as predicted by NESTLE NM with and without ADF. Larger differences are noted due to just utilization of ADFs than noted in Figure 2, with NM without ADF rolling the channel relative power distribution from the core exterior to the core edge. The better agreement with NESTLE FDM occurs because utilization of the fuel-reflector interface ADF causes a power roll that offsets the finite difference truncation error induced power roll.

Figure 4 shows the total prompt thermal power as a function of time as predicted by the three different spatial discretization treatments. Note that the fission source term in NESTLE is scaled by $1/k_{eff}$, so the differences in the predicted initial $k_{eff}$ due to spatial discretization differences are effectively removed. Up to the time of the power peak, all three spatial treatments predict a similar power transient. After the time of the peak power, NESTLE FDM predicts the lowest powers, with NESTLE NM with and without ADF predicting similar powers. The plant data indicates that the peak reactor power reached is approximately 110%FP. NESTLE FDM, NESTLE NM without ADF, and NESTLE NM with ADF predict peak core powers of 111.05%FP, 110.60%FP and 110.83%FP, respectively, resulting in about 0.60-1.05 %FP over prediction of the experimentally inferred peak core power. As noted earlier, these predictions utilize the CERBERUS/SOPHT-G2 predicted thermal-hydraulic conditions and time of SDS1 plant trip signal. If NESTLE predictions are utilized to determine when the SDS1 plant trip signal occurs, it is determined to occur earlier versus that predicted by CERBERUS/SOPHT-G2. Using this earlier trip time, the NESTLE predictions of peak core power would be reduced since SOR insertion would occur earlier, improving agreement with plant data.

To assure that the temporal discretization error is not noticeable impacting the total prompt thermal power transient predicted, the time-step sizes were refined to ½, ¼, and 1/8 of the original time-step sizes. The original time-step sizes were taken from the CERBERUS simulation. The transient was then re-simulated using NESTLE NM with ADF obtaining thermal-hydraulics conditions and control devices' positions at the new discrete time values that result from time-step size refinement via linear interpolation. Since time-step size refinement results in SOR and other device insertions no longer aligning with spatial node boundaries, cross-sections homogenization of uncontrolled and controlled values was necessary, completed within NESTLE by volume weighting. Note that volume weighting will introduce a rod cusp effect. Figure 5 presents the resulting total prompt thermal power transient. The peak powers predicted are 110.83%FP, 111.23%FP, 111.35%FP, and 111.40%FP for the original, ½, ¼, and 1/8, respectively, time-step sizes. The peak powers predicted for all the refined time-steps are much closer to each other compared with the original time-step sizes. The refined time-steps also all predict the peak to occur at 1.3238 sec, while the original time-steps predicts it to occur at 1.2855 sec.

Further examination of Figure 5 indicates that for times after the time of the peak power, the results for the original and the halved time-steps are not converged and time-step size refinement results in higher total prompt thermal power predictions. Rod cusping effects may be contributing to the lack of convergence of the peak power with time-step size refinement; however, the noted behaviour is inconsistent with the rod cusp effect which over-estimates rod worth in mid-node insertion positions. Likely what explains the observed behaviour is that NESTLE employs a fully implicit treatment in approximating the temporal component. This implies that the core state at the end of a time-step is assumed to exist over the entire time-step. During SOR insertion, this implies deeper SOR insertions than actually occur, resulting in quicker negative reactivity insertion and hence a more rapid decrease in the total prompt thermal power with time. As the time-step size is refined, these effects are minimized, consistent with the behaviour noted in Figure 5. This may perhaps help to explain the observation made above that both the peak power and time of peak power increase with time-step size refinement.

These results for the time-step size refinement indicate that the original time-step sizes are not sufficiently refined for usage by NESTLE. As the time-step sizes were refined to $1/8^{th}$ of their initial values, as noted above the peak power increased by 0.57%FP. The differences of the predicted channel relative power distributions at the time of peak power for the three different spatial discretization treatments are very similar to what is observed at the start of the transient, indicating that while at substantial core power levels the kinetic effects do not influence the quality of the comparisons. Note that some spatial redistribution of the predicted channel relative power distributions have occurred at the time of peak power due to thermal-hydraulic feedback and the partial insertion of the SORs.

**Coolant Density Sensitivity Study**

The coolant density radial gradient within the bundle has been considered in adjusting the SOPHT-G2 generated data with a correction factor (called "WIMS-ASSERT" correction) in a previous study of the accident [1]. The appropriateness of this correction has not been assessed in this project, only the sensitivity to uncertainty in predicted node averaged homogenized coolant density has been studied. This has been accomplished by modifying each node averaged coolant density by multiplying the decrease in the density, *i.e.* the difference between the density at the initial time and each time-step, by a multiplier (0.1-0.5) and subtracting it from the density at that time-step. For example, a 0.1 multiplier equates to a 10% larger decrease in the change of the coolant density from its initial density. The greater decrease in coolant density as the transient progresses increases the coolant's positive reactivity insertion. The original core volume averaged coolant density at the time of the peak power is 0.73603 gm/cc. The modified core averaged coolant densities at the time of the peak power for multipliers of 0.1, 0.2, 0.3, 0.4, and 0.5 are 0.73234, 0.72865, 0.72496, 0.72127 and 0.71758 gm/cc, respectively. Figure 6 shows the total prompt thermal power versus time as predicted by NESTLE NM without ADF. As the density is reduced by using the multipliers of 0.1, 0.2, 0.3, 0.4, and 0.5, the predicted peak prompt thermal powers are 111.84%FP, 112.85%FP, 113.93%FP, 114.96%FP and 116.03%FP, respectively. Note that without any changes to the densities, the peak prompt thermal power is 110.83%FP. This indicates that as the multiplier is increased by 0.1, equivalent to the core averaged coolant density at the time of the peak power decreasing by 0.0037 gm/cc, the peak prompt thermal power increases approximately by 1%FP. Note that in reality, the more severe transient would cause an earlier power rate trip and hence earlier SOR insertion, reducing the peak power predicted.

Similar sensitivity studies were done on the coolant temperature and fuel temperature with results indicating little change in the total prompt thermal power and the peak. Coolant temperature and fuel temperature perturbations hardly impacted the predicted transient behavior since neither of these core properties change significantly for this short-lived transient.

**Conclusions**

The spatial discretization treatment in the NESTLE core simulator is observed to have only a minor effect on the core reactivity as indicated by $k_{eff}$ and the total prompt thermal power transient for the

Gentilly-2 event. Utilization of a NM without ADFs does cause a noticeable channel relative power distribution roll from the core edge to interior when contrasted with the FDM, but adding the utilization of ADFs with the NM causes the reverse power roll, minimizing differences in channel relative powers to less than 0.04 for NESTLE NM with ADF versus NESTLE FDM. One would assume that the NM with ADF treatment is most accurate, but this must be verified via benchmark calculations and plant measurements. The sensitivity study demonstrated the importance of the coolant density-change induced reactivity in a CANDU core, even for such a mild transient.

## References


[1] A. Baudouin, K. Joober, T. Sissaoui, H. Chow and G. Hotte, "Coolant Void Reactivity Transient in a Gentilly-2 Loss of Flow Event," Canadian Nuclear Society Annual Meeting, Toronto, 2001.

[2] P. J. Turinsky, R. M. K. Al-Chalabi, P. Engrand, H. N. Sarsour, F. X. Faure and W. Guo, "NESTLE: A Few-Group Neutron Diffusion Solver Utilizing the Nodal Expansion Method for Eigenvalue, Adjoint, Fixed-Source Steady-State and Transient Problems," EGG-NRE-11406, Idaho National Engineering Laboratory (1994).

[3] Casal J J, Stamm'ler R J J, Villarino E A and Ferri A A, "HELIOS: Geometric Capabilities of a New Fuel-Assembly Program," Intl Topical Meeting on Advances in Mathematics, Computations, and Reactor Physics, Pittsburgh, Pennsylvania, April 28-May 2, 1991,Vol. 2, p. 10.2.1 1-13 (1991).

[4] R. Roy, G. Marleau, J. Tajmouati and D. Rozon, "Modeling of CANDU Reactivity Control Devices with the Lattice Code DRAGON," Ann. Nucl. Energy, **21**, 115 (1994).

**Table I. Original time step sizes used for the base case**

| Time Span That Time-step Size Is Applied To | | Time-step Size (sec) |
|---|---|---|
| **Starting Time (sec)** | **Ending Time (sec)** | |
| 0.0 | 0.8 | 0.1 |
| 0.8 | 1.1474 | 0.132-0.2154 |
| 1.1474 | 2.8844 | 0.0361-0.0953 |
| 2.8844 | 4.0 | 0.1024-0.2038 |

**Figure 1. Full core mesh layout for axial span of core**
**(2 denotes fuel nodes, 1 denotes reflector nodes, and 0 denotes null nodes)**

```
0 0 0 0 0 0 0 0 0 0 0 0 0 0 0 0 0 0 0 0 1 1 1 1 1 1 0 0 0 0 0 0 0 0 0 0 0 0 0 0 0 0 0 0 0 0
0 0 0 0 0 0 0 0 0 0 0 0 0 0 1 1 1 1 1 1 1 1 1 1 1 1 1 1 1 1 1 1 0 0 0 0 0 0 0 0 0 0 0 0 0 0
0 0 0 0 0 0 0 0 0 0 0 1 1 1 1 1 1 1 1 1 1 1 1 1 1 1 1 1 1 1 1 1 1 1 1 0 0 0 0 0 0 0 0 0 0 0
0 0 0 0 0 0 0 0 0 1 1 1 1 1 1 1 1 1 1 1 1 1 1 1 1 1 1 1 1 1 1 1 1 1 1 1 1 0 0 0 0 0 0 0 0 0
0 0 0 0 0 0 0 1 1 1 1 1 1 1 1 1 1 2 2 2 2 2 2 2 2 2 2 2 2 1 1 1 1 1 1 1 1 1 1 0 0 0 0 0 0 0
0 0 0 0 0 1 1 1 1 1 1 2 2 2 2 2 2 2 2 2 2 2 2 2 2 2 2 2 2 2 2 2 2 2 2 1 1 1 1 1 1 0 0 0 0 0
0 0 0 0 1 1 1 1 1 2 2 2 2 2 2 2 2 2 2 2 2 2 2 2 2 2 2 2 2 2 2 2 2 2 2 2 2 1 1 1 1 1 0 0 0 0
0 0 0 1 1 1 1 2 2 2 2 2 2 2 2 2 2 2 2 2 2 2 2 2 2 2 2 2 2 2 2 2 2 2 2 2 2 2 2 1 1 1 1 0 0 0
0 0 1 1 1 2 2 2 2 2 2 2 2 2 2 2 2 2 2 2 2 2 2 2 2 2 2 2 2 2 2 2 2 2 2 2 2 2 2 2 2 1 1 1 0 0
0 0 1 1 1 2 2 2 2 2 2 2 2 2 2 2 2 2 2 2 2 2 2 2 2 2 2 2 2 2 2 2 2 2 2 2 2 2 2 2 2 1 1 1 0 0
0 0 1 1 1 2 2 2 2 2 2 2 2 2 2 2 2 2 2 2 2 2 2 2 2 2 2 2 2 2 2 2 2 2 2 2 2 2 2 2 2 1 1 1 0 0
0 1 1 1 2 2 2 2 2 2 2 2 2 2 2 2 2 2 2 2 2 2 2 2 2 2 2 2 2 2 2 2 2 2 2 2 2 2 2 2 2 2 1 1 1 0
0 1 1 1 2 2 2 2 2 2 2 2 2 2 2 2 2 2 2 2 2 2 2 2 2 2 2 2 2 2 2 2 2 2 2 2 2 2 2 2 2 2 1 1 1 0
0 1 1 2 2 2 2 2 2 2 2 2 2 2 2 2 2 2 2 2 2 2 2 2 2 2 2 2 2 2 2 2 2 2 2 2 2 2 2 2 2 2 2 1 1 0
0 1 1 2 2 2 2 2 2 2 2 2 2 2 2 2 2 2 2 2 2 2 2 2 2 2 2 2 2 2 2 2 2 2 2 2 2 2 2 2 2 2 2 1 1 0
1 1 1 2 2 2 2 2 2 2 2 2 2 2 2 2 2 2 2 2 2 2 2 2 2 2 2 2 2 2 2 2 2 2 2 2 2 2 2 2 2 2 2 1 1 1
1 1 1 2 2 2 2 2 2 2 2 2 2 2 2 2 2 2 2 2 2 2 2 2 2 2 2 2 2 2 2 2 2 2 2 2 2 2 2 2 2 2 2 1 1 1
1 1 1 2 2 2 2 2 2 2 2 2 2 2 2 2 2 2 2 2 2 2 2 2 2 2 2 2 2 2 2 2 2 2 2 2 2 2 2 2 2 2 2 1 1 1
1 1 1 2 2 2 2 2 2 2 2 2 2 2 2 2 2 2 2 2 2 2 2 2 2 2 2 2 2 2 2 2 2 2 2 2 2 2 2 2 2 2 2 1 1 1
0 1 1 2 2 2 2 2 2 2 2 2 2 2 2 2 2 2 2 2 2 2 2 2 2 2 2 2 2 2 2 2 2 2 2 2 2 2 2 2 2 2 2 1 1 0
0 1 1 2 2 2 2 2 2 2 2 2 2 2 2 2 2 2 2 2 2 2 2 2 2 2 2 2 2 2 2 2 2 2 2 2 2 2 2 2 2 2 2 1 1 0
0 1 1 1 2 2 2 2 2 2 2 2 2 2 2 2 2 2 2 2 2 2 2 2 2 2 2 2 2 2 2 2 2 2 2 2 2 2 2 2 2 2 1 1 1 0
0 1 1 1 2 2 2 2 2 2 2 2 2 2 2 2 2 2 2 2 2 2 2 2 2 2 2 2 2 2 2 2 2 2 2 2 2 2 2 2 2 2 1 1 1 0
0 0 1 1 1 2 2 2 2 2 2 2 2 2 2 2 2 2 2 2 2 2 2 2 2 2 2 2 2 2 2 2 2 2 2 2 2 2 2 2 2 1 1 1 0 0
0 0 1 1 1 2 2 2 2 2 2 2 2 2 2 2 2 2 2 2 2 2 2 2 2 2 2 2 2 2 2 2 2 2 2 2 2 2 2 2 2 1 1 1 0 0
0 0 1 1 1 2 2 2 2 2 2 2 2 2 2 2 2 2 2 2 2 2 2 2 2 2 2 2 2 2 2 2 2 2 2 2 2 2 2 2 2 1 1 1 0 0
0 0 0 1 1 1 1 2 2 2 2 2 2 2 2 2 2 2 2 2 2 2 2 2 2 2 2 2 2 2 2 2 2 2 2 2 2 2 2 1 1 1 1 0 0 0
0 0 0 0 1 1 1 1 1 2 2 2 2 2 2 2 2 2 2 2 2 2 2 2 2 2 2 2 2 2 2 2 2 2 2 2 2 1 1 1 1 1 0 0 0 0
0 0 0 0 0 1 1 1 1 1 1 2 2 2 2 2 2 2 2 2 2 2 2 2 2 2 2 2 2 2 2 2 2 2 2 1 1 1 1 1 1 0 0 0 0 0
0 0 0 0 0 0 0 1 1 1 1 1 1 1 1 1 1 2 2 2 2 2 2 2 2 2 2 2 2 1 1 1 1 1 1 1 1 1 1 0 0 0 0 0 0 0
0 0 0 0 0 0 0 0 0 1 1 1 1 1 1 1 1 1 1 1 1 1 1 1 1 1 1 1 1 1 1 1 1 1 1 1 1 0 0 0 0 0 0 0 0 0
0 0 0 0 0 0 0 0 0 0 0 1 1 1 1 1 1 1 1 1 1 1 1 1 1 1 1 1 1 1 1 1 1 1 1 0 0 0 0 0 0 0 0 0 0 0
0 0 0 0 0 0 0 0 0 0 0 0 0 0 1 1 1 1 1 1 1 1 1 1 1 1 1 1 1 1 1 1 0 0 0 0 0 0 0 0 0 0 0 0 0 0
0 0 0 0 0 0 0 0 0 0 0 0 0 0 0 0 0 0 0 0 1 1 1 1 1 1 0 0 0 0 0 0 0 0 0 0 0 0 0 0 0 0 0 0 0 0
```

**Figure 2. Steady state channel power distribution for NESTLE NM and NESTLE FDM**

**NESTLE NM w/ ADF**
**NESTLE FDM**
**Diff**

```
                                                  0.64  0.66  0.69  0.67  0.61  0.59
                                                  0.66  0.69  0.71  0.70  0.63  0.62A
                                                 -0.02 -0.03 -0.02 -0.03 -0.02 -0.03A

                                  0.56  0.70  0.80  0.85  0.89  0.88  0.81  0.83  0.78  0.74  0.62  0.46
                                  0.58  0.71  0.81  0.86  0.91  0.90  0.83  0.85  0.80  0.75  0.63  0.47B
                                 -0.02 -0.01 -0.01 -0.02 -0.02 -0.02 -0.02 -0.02 -0.02 -0.01 -0.01 -0.01B

                            0.59  0.77  0.88  0.92  0.99  1.03  1.04  1.02  0.95  0.98  0.91  0.77  0.61  0.54
                            0.60  0.78  0.90  0.93  1.00  1.03  1.04  1.02  0.96  0.99  0.92  0.78  0.63  0.56C
                           -0.01 -0.01 -0.02 -0.01 -0.01  0.00  0.00  0.00 -0.01 -0.01 -0.01 -0.01 -0.02 -0.02C

                      0.69  0.82  0.88  1.02  1.03  1.10  1.17  1.06  1.11  1.11  1.04  0.99  0.89  0.78  0.69  0.53
                      0.70  0.83  0.88  1.01  1.01  1.09  1.16  1.05  1.11  1.12  1.04  0.99  0.89  0.79  0.70  0.55D
                     -0.01 -0.01  0.00  0.01  0.02  0.01  0.01  0.01  0.00 -0.01  0.00  0.00  0.00 -0.01 -0.01 -0.02D

                0.66  0.84  0.95  1.09  1.14  1.22  1.24  1.20  1.17  1.10  1.13  1.16  1.12  1.07  0.98  0.78  0.66  0.57
                0.66  0.84  0.95  1.09  1.13  1.20  1.22  1.18  1.15  1.08  1.12  1.16  1.12  1.07  0.98  0.79  0.67  0.57E
                0.00  0.00  0.00  0.00  0.01  0.02  0.02  0.02  0.02  0.02  0.01  0.00  0.00  0.00  0.00 -0.01 -0.01  0.00E

                0.82  0.98  1.10  1.16  1.25  1.29  1.27  1.19  1.19  1.10  1.17  1.11  1.13  1.09  1.08  0.95  0.82  0.71
                0.82  0.98  1.10  1.15  1.23  1.27  1.24  1.16  1.15  1.07  1.14  1.08  1.11  1.08  1.08  0.96  0.83  0.72F
                0.00  0.00  0.00  0.01  0.02  0.02  0.03  0.03  0.04  0.03  0.03  0.02  0.02  0.01  0.00 -0.01 -0.01 -0.01F

          0.73  0.92  1.02  1.10  1.20  1.13  1.28  1.28  1.25  1.17  1.17  1.16  1.17  1.19  1.20  1.10  1.07  0.94  0.81  0.67
          0.73  0.92  1.00  1.08  1.17  1.10  1.25  1.25  1.22  1.14  1.14  1.14  1.16  1.17  1.18  1.09  1.07  0.95  0.82  0.68G
          0.00  0.00  0.02  0.02  0.03  0.03  0.03  0.03  0.03  0.03  0.03  0.02  0.01  0.02  0.02  0.01  0.00 -0.01 -0.01 -0.01G

          0.82  1.03  1.15  1.16  1.16  1.16  1.23  1.20  1.24  1.23  1.21  1.10  1.20  1.22  1.18  1.20  1.15  1.08  0.93  0.73
          0.82  1.03  1.14  1.13  1.13  1.13  1.20  1.16  1.21  1.21  1.19  1.07  1.18  1.21  1.16  1.19  1.15  1.10  0.95  0.74H
          0.00  0.00  0.01  0.03  0.03  0.03  0.03  0.04  0.03  0.02  0.02  0.02  0.02  0.01  0.02  0.01  0.00 -0.02 -0.02 -0.01H

    0.61  0.88  1.07  1.17  1.20  1.13  1.21  1.24  1.17  1.24  1.22  1.15  1.17  1.13  1.19  1.20  1.21  1.13  1.15  0.96  0.85  0.63
    0.60  0.88  1.06  1.15  1.17  1.10  1.18  1.21  1.13  1.21  1.19  1.12  1.13  1.10  1.16  1.18  1.20  1.13  1.15  0.97  0.87  0.64J
    0.01  0.00  0.01  0.02  0.03  0.03  0.03  0.03  0.03  0.03  0.03  0.03  0.04  0.03  0.03  0.02  0.01  0.00  0.00 -0.01 -0.02 -0.01J

    0.66  0.86  1.05  1.15  1.20  1.15  1.20  1.19  1.23  1.21  1.23  1.22  1.20  1.20  1.22  1.22  1.19  1.19  1.19  1.02  0.90  0.70
    0.65  0.86  1.03  1.13  1.16  1.12  1.17  1.16  1.19  1.19  1.20  1.20  1.18  1.18  1.20  1.20  1.16  1.18  1.19  1.04  0.94  0.72K
    0.01  0.00  0.02  0.02  0.04  0.03  0.03  0.03  0.04  0.02  0.03  0.02  0.02  0.02  0.02  0.02  0.02  0.01  0.00 -0.02 -0.04 -0.02K

    0.71  0.92  1.11  1.13  1.21  1.11  1.21  1.22  1.22  1.16  1.13  1.18  1.16  1.14  1.13  1.23  1.25  1.25  1.22  1.11  0.93  0.70
    0.72  0.93  1.10  1.10  1.18  1.08  1.18  1.19  1.19  1.13  1.09  1.15  1.13  1.12  1.11  1.22  1.25  1.26  1.24  1.13  0.97  0.72L
   -0.01 -0.01  0.01  0.03  0.03  0.03  0.03  0.03  0.03  0.03  0.04  0.03  0.03  0.02  0.02  0.01  0.00 -0.01 -0.02 -0.02 -0.04 -0.02L

    0.68  0.93  1.11  1.19  1.24  1.16  1.16  1.11  1.18  1.20  1.19  1.19  1.20  1.18  1.13  1.22  1.22  1.18  1.15  1.13  0.88  0.72
    0.68  0.95  1.11  1.18  1.22  1.13  1.12  1.08  1.14  1.17  1.16  1.17  1.18  1.16  1.12  1.21  1.22  1.18  1.16  1.14  0.90  0.74M
   -0.01 -0.02  0.00  0.01  0.02  0.03  0.04  0.03  0.04  0.03  0.03  0.02  0.02  0.02  0.01  0.01  0.00  0.00 -0.01 -0.01 -0.02 -0.02M

    0.66  0.87  1.05  1.22  1.23  1.24  1.24  1.17  1.15  1.12  1.14  1.15  1.21  1.15  1.13  1.22  1.19  1.21  1.12  1.11  0.93  0.69
    0.67  0.88  1.04  1.20  1.20  1.21  1.21  1.14  1.12  1.09  1.10  1.12  1.18  1.13  1.11  1.21  1.19  1.21  1.13  1.12  0.96  0.72N
   -0.01 -0.01  0.01  0.02  0.03  0.03  0.03  0.02  0.03  0.03  0.04  0.03  0.03  0.02  0.02  0.01  0.00  0.00 -0.01 -0.01 -0.03 -0.03N

    0.56  0.78  1.03  1.17  1.27  1.30  1.21  1.26  1.25  1.21  1.21  1.13  1.20  1.16  1.20  1.23  1.13  1.21  1.13  1.06  0.87  0.65
    0.57  0.78  1.03  1.16  1.26  1.29  1.18  1.24  1.23  1.19  1.19  1.11  1.18  1.15  1.19  1.22  1.13  1.22  1.14  1.08  0.90  0.68O
   -0.01  0.00  0.00  0.01  0.01  0.01  0.03  0.02  0.02  0.02  0.02  0.02  0.02  0.01  0.01  0.01  0.00 -0.01 -0.01 -0.02 -0.03 -0.03O

          0.71  0.88  1.11  1.17  1.25  1.27  1.29  1.24  1.26  1.24  1.23  1.19  1.21  1.23  1.22  1.15  1.13  1.10  0.97  0.73
          0.71  0.89  1.10  1.16  1.24  1.26  1.28  1.22  1.25  1.23  1.22  1.18  1.21  1.24  1.23  1.16  1.14  1.13  1.00  0.75P
          0.00 -0.01  0.01  0.01  0.01  0.01  0.01  0.02  0.01  0.01  0.01  0.01  0.00 -0.01 -0.01 -0.01 -0.01 -0.03 -0.03 -0.02P

          0.66  0.82  0.95  1.11  1.20  1.19  1.22  1.25  1.24  1.22  1.16  1.11  1.18  1.16  1.14  1.09  1.06  0.95  0.85  0.67
          0.67  0.82  0.95  1.10  1.19  1.18  1.21  1.23  1.23  1.21  1.15  1.10  1.17  1.15  1.14  1.10  1.08  0.97  0.87  0.69Q
         -0.01  0.00  0.00  0.01  0.01  0.01  0.01  0.02  0.01  0.01  0.01  0.01  0.01  0.01  0.00 -0.01 -0.02 -0.02 -0.02 -0.02Q

                0.74  0.87  0.93  1.09  1.11  1.19  1.21  1.15  1.08  1.14  1.10  1.16  1.14  1.12  1.02  0.94  0.81  0.72
                0.75  0.88  0.92  1.09  1.11  1.18  1.20  1.14  1.06  1.13  1.10  1.17  1.15  1.13  1.04  0.96  0.84  0.75R
               -0.01 -0.01  0.01  0.00  0.00  0.01  0.01  0.01  0.02  0.01  0.00 -0.01 -0.01 -0.01 -0.02 -0.02 -0.03 -0.03R

                0.54  0.72  0.85  0.98  1.01  1.15  1.18  1.16  1.06  1.07  1.08  1.12  1.04  1.03  0.88  0.80  0.64  0.54
                0.55  0.74  0.87  0.99  1.03  1.16  1.20  1.17  1.07  1.09  1.11  1.14  1.06  1.05  0.90  0.82  0.67  0.56S
               -0.01 -0.02 -0.02 -0.01 -0.02 -0.01 -0.02 -0.01 -0.01 -0.02 -0.03 -0.02 -0.02 -0.02 -0.02 -0.02 -0.03 -0.02S

                      0.55  0.70  0.83  0.90  1.03  1.03  1.06  0.96  1.02  1.04  0.98  0.94  0.89  0.71  0.63  0.49
                      0.58  0.74  0.87  0.92  1.05  1.04  1.08  0.97  1.04  1.07  1.01  0.97  0.91  0.74  0.66  0.53T
                     -0.03 -0.04 -0.04 -0.02 -0.02 -0.01 -0.02 -0.01 -0.02 -0.03 -0.03 -0.03 -0.02 -0.03 -0.03 -0.04T

                            0.49  0.63  0.75  0.86  0.92  0.93  0.91  0.87  0.89  0.87  0.80  0.70  0.57  0.43
                            0.52  0.66  0.79  0.90  0.95  0.96  0.94  0.90  0.92  0.91  0.84  0.74  0.61  0.46U
                           -0.03 -0.03 -0.04 -0.04 -0.03 -0.03 -0.03 -0.03 -0.03 -0.04 -0.04 -0.04 -0.04 -0.03U

                                  0.40  0.54  0.62  0.69  0.72  0.71  0.72  0.68  0.66  0.57  0.45  0.35
                                  0.44  0.57  0.65  0.72  0.76  0.74  0.76  0.73  0.70  0.60  0.48  0.39V
                                 -0.04 -0.03 -0.03 -0.03 -0.04 -0.04 -0.04 -0.05 -0.04 -0.03 -0.03 -0.04V

                                                  0.45  0.48  0.49  0.49  0.46  0.41
                                                  0.48  0.52  0.53  0.53  0.50  0.45W
                                                 -0.03 -0.04 -0.04 -0.04 -0.04 -0.04W
```

**Figure 3. Steady state channel power distribution for NESTLE NM with and without ADFs**

**NESTLE NM w/ ADF**
**NESTLE NM w/o ADF**
**Diff**

```
                                                  0.64  0.66  0.69  0.67  0.61  0.59
                                                  0.70  0.72  0.74  0.73  0.67  0.66A
                                                 -0.06 -0.06 -0.06 -0.06 -0.06 -0.07A

                                    0.56  0.70  0.80  0.85  0.89  0.88  0.81  0.83  0.78  0.74  0.62  0.46
                                    0.62  0.76  0.85  0.89  0.92  0.91  0.85  0.86  0.82  0.78  0.67  0.51B
                                   -0.06 -0.06 -0.05 -0.04 -0.03 -0.03 -0.04 -0.03 -0.04 -0.04 -0.05 -0.05B

                              0.59  0.77  0.88  0.92  0.99  1.03  1.04  1.02  0.95  0.98  0.91  0.77  0.61  0.54
                              0.65  0.81  0.92  0.95  1.02  1.05  1.04  1.03  0.98  1.00  0.93  0.80  0.65  0.59C
                             -0.06 -0.04 -0.04 -0.03 -0.03 -0.02  0.00 -0.01 -0.03 -0.02 -0.02 -0.03 -0.04 -0.05C

                        0.69  0.82  0.88  1.02  1.03  1.10  1.17  1.06  1.11  1.11  1.04  0.99  0.89  0.78  0.69  0.53
                        0.75  0.85  0.91  1.04  1.04  1.11  1.16  1.06  1.11  1.12  1.05  1.01  0.91  0.81  0.73  0.58D
                       -0.06 -0.03 -0.03 -0.02 -0.01 -0.01  0.01  0.00 -0.01 -0.01 -0.01 -0.02 -0.02 -0.03 -0.04 -0.05D

                  0.66  0.84  0.95  1.09  1.14  1.22  1.24  1.20  1.17  1.10  1.13  1.16  1.12  1.07  0.98  0.78  0.66  0.57
                  0.73  0.88  0.98  1.10  1.15  1.22  1.23  1.19  1.15  1.09  1.12  1.16  1.12  1.08  0.99  0.81  0.70  0.62E
                 -0.07 -0.04 -0.03 -0.02 -0.01  0.00  0.01  0.01  0.02  0.01  0.01  0.00  0.00 -0.01 -0.01 -0.03 -0.04 -0.05E

                  0.82  0.98  1.10  1.16  1.25  1.29  1.27  1.19  1.19  1.10  1.17  1.11  1.13  1.09  1.08  0.95  0.82  0.71
                  0.88  1.01  1.11  1.16  1.23  1.26  1.25  1.16  1.16  1.08  1.15  1.10  1.12  1.09  1.08  0.97  0.85  0.77F
                 -0.06 -0.03 -0.01  0.00  0.02  0.03  0.02  0.03  0.03  0.02  0.02  0.01  0.01  0.00  0.00 -0.02 -0.03 -0.06F

            0.73  0.92  1.02  1.10  1.20  1.13  1.28  1.28  1.25  1.17  1.17  1.16  1.17  1.19  1.20  1.10  1.07  0.94  0.81  0.67
            0.80  0.96  1.04  1.11  1.19  1.12  1.25  1.25  1.21  1.14  1.14  1.14  1.15  1.17  1.18  1.10  1.08  0.97  0.86  0.74G
           -0.07 -0.04 -0.02 -0.01  0.01  0.01  0.03  0.03  0.04  0.03  0.03  0.02  0.02  0.02  0.02  0.00 -0.01 -0.03 -0.05 -0.07G

            0.82  1.03  1.15  1.16  1.16  1.16  1.23  1.20  1.24  1.23  1.21  1.10  1.20  1.22  1.18  1.20  1.15  1.08  0.93  0.73
            0.87  1.05  1.16  1.15  1.14  1.14  1.20  1.16  1.20  1.19  1.17  1.07  1.16  1.19  1.16  1.19  1.16  1.11  0.97  0.79H
           -0.05 -0.02 -0.01  0.01  0.02  0.02  0.03  0.04  0.04  0.04  0.04  0.03  0.03  0.03  0.02  0.01 -0.01 -0.03 -0.05 -0.06H

  0.61  0.88  1.07  1.17  1.20  1.13  1.21  1.24  1.17  1.24  1.22  1.15  1.17  1.13  1.19  1.20  1.21  1.13  1.15  0.96  0.85  0.63
  0.67  0.91  1.09  1.17  1.19  1.11  1.18  1.20  1.13  1.19  1.17  1.11  1.12  1.10  1.16  1.17  1.19  1.14  1.17  1.00  0.90  0.71J
 -0.06 -0.03 -0.02  0.00  0.01  0.02  0.03  0.04  0.04  0.05  0.05  0.04  0.05  0.03  0.03  0.03  0.02 -0.01 -0.02 -0.04 -0.05 -0.08J

  0.66  0.86  1.05  1.15  1.20  1.15  1.20  1.19  1.23  1.21  1.23  1.22  1.20  1.20  1.22  1.22  1.19  1.19  1.19  1.02  0.90  0.70
  0.71  0.89  1.07  1.15  1.17  1.12  1.17  1.15  1.17  1.16  1.17  1.17  1.15  1.16  1.18  1.19  1.17  1.19  1.21  1.06  0.95  0.77K
 -0.05 -0.03 -0.02  0.00  0.03  0.03  0.03  0.04  0.06  0.05  0.06  0.05  0.05  0.04  0.04  0.03  0.02  0.00 -0.02 -0.04 -0.05 -0.07K

  0.71  0.92  1.11  1.13  1.21  1.11  1.21  1.22  1.22  1.16  1.13  1.18  1.16  1.14  1.13  1.23  1.25  1.25  1.22  1.11  0.93  0.70
  0.77  0.94  1.12  1.12  1.19  1.09  1.17  1.17  1.17  1.11  1.08  1.13  1.12  1.11  1.10  1.20  1.23  1.25  1.23  1.14  0.97  0.77L
 -0.06 -0.02 -0.01  0.01  0.02  0.02  0.04  0.05  0.05  0.05  0.05  0.05  0.04  0.03  0.03  0.03  0.02  0.00 -0.01 -0.03 -0.04 -0.07L

  0.68  0.93  1.11  1.19  1.24  1.16  1.16  1.11  1.18  1.20  1.19  1.19  1.20  1.18  1.13  1.22  1.22  1.18  1.15  1.13  0.88  0.72
  0.73  0.96  1.12  1.19  1.22  1.14  1.12  1.07  1.12  1.13  1.13  1.14  1.15  1.14  1.10  1.19  1.21  1.18  1.17  1.16  0.92  0.79M
 -0.05 -0.03 -0.01  0.00  0.02  0.02  0.04  0.04  0.06  0.07  0.06  0.05  0.05  0.04  0.03  0.03  0.01  0.00 -0.02 -0.03 -0.04 -0.07M

  0.66  0.87  1.05  1.22  1.23  1.24  1.24  1.17  1.15  1.12  1.14  1.15  1.21  1.15  1.13  1.22  1.19  1.21  1.12  1.11  0.93  0.69
  0.71  0.90  1.06  1.20  1.20  1.20  1.19  1.13  1.10  1.07  1.08  1.10  1.15  1.11  1.09  1.19  1.18  1.21  1.14  1.13  0.97  0.76N
 -0.05 -0.03 -0.01  0.02  0.03  0.04  0.05  0.04  0.05  0.04  0.05  0.05  0.06  0.04  0.04  0.03  0.01  0.00 -0.02 -0.02 -0.04 -0.07N

  0.56  0.78  1.03  1.17  1.27  1.30  1.21  1.26  1.25  1.21  1.21  1.13  1.20  1.16  1.20  1.23  1.13  1.21  1.13  1.06  0.87  0.65
  0.62  0.81  1.03  1.16  1.25  1.26  1.17  1.20  1.19  1.16  1.15  1.09  1.14  1.13  1.17  1.20  1.12  1.21  1.14  1.09  0.92  0.72O
 -0.06 -0.03  0.00  0.01  0.02  0.04  0.04  0.06  0.06  0.05  0.06  0.04  0.06  0.03  0.03  0.03  0.01  0.00 -0.01 -0.03 -0.05 -0.07O

            0.71  0.88  1.11  1.17  1.25  1.27  1.29  1.24  1.26  1.24  1.23  1.19  1.21  1.23  1.22  1.15  1.13  1.10  0.97  0.73
            0.75  0.90  1.10  1.15  1.22  1.23  1.24  1.19  1.21  1.19  1.17  1.14  1.17  1.19  1.20  1.14  1.13  1.12  1.01  0.80P
           -0.04 -0.02  0.01  0.02  0.03  0.04  0.05  0.05  0.05  0.05  0.06  0.05  0.04  0.04  0.02  0.01  0.00 -0.02 -0.04 -0.07P

            0.66  0.82  0.95  1.11  1.20  1.19  1.22  1.25  1.24  1.22  1.16  1.11  1.18  1.16  1.14  1.09  1.06  0.95  0.85  0.67
            0.71  0.84  0.95  1.09  1.17  1.16  1.18  1.19  1.19  1.17  1.11  1.08  1.15  1.13  1.12  1.08  1.07  0.98  0.89  0.74Q
           -0.05 -0.02  0.00  0.02  0.03  0.03  0.04  0.06  0.05  0.05  0.05  0.03  0.03  0.03  0.02  0.01 -0.01 -0.03 -0.04 -0.07Q

                  0.74  0.87  0.93  1.09  1.11  1.19  1.21  1.15  1.08  1.14  1.10  1.16  1.14  1.12  1.02  0.94  0.81  0.72
                  0.77  0.88  0.92  1.07  1.09  1.15  1.17  1.12  1.04  1.09  1.07  1.13  1.12  1.10  1.02  0.95  0.84  0.78R
                 -0.03 -0.01  0.01  0.02  0.02  0.04  0.04  0.03  0.04  0.05  0.03  0.03  0.02  0.02  0.00 -0.01 -0.03 -0.06R

                  0.54  0.72  0.85  0.98  1.01  1.15  1.18  1.16  1.06  1.07  1.08  1.12  1.04  1.03  0.88  0.80  0.64  0.54
                  0.58  0.74  0.86  0.97  1.00  1.12  1.15  1.12  1.03  1.05  1.07  1.10  1.02  1.02  0.89  0.81  0.68  0.60S
                 -0.04 -0.02 -0.01  0.01  0.01  0.03  0.03  0.04  0.03  0.02  0.01  0.02  0.02  0.01 -0.01 -0.01 -0.04 -0.06S

                        0.55  0.70  0.83  0.90  1.03  1.03  1.06  0.96  1.02  1.04  0.98  0.94  0.89  0.71  0.63  0.49
                        0.59  0.72  0.84  0.89  1.02  1.01  1.04  0.94  1.00  1.02  0.98  0.94  0.88  0.73  0.65  0.54T
                       -0.04 -0.02 -0.01  0.01  0.01  0.02  0.02  0.02  0.02  0.02  0.00  0.00  0.01 -0.02 -0.02 -0.05T

                              0.49  0.63  0.75  0.86  0.92  0.93  0.91  0.87  0.89  0.87  0.80  0.70  0.57  0.43
                              0.52  0.64  0.76  0.86  0.91  0.92  0.89  0.87  0.89  0.87  0.81  0.71  0.59  0.47U
                             -0.03 -0.01 -0.01  0.00  0.01  0.01  0.02  0.00  0.00  0.00 -0.01 -0.01 -0.02 -0.04U

                                    0.40  0.54  0.62  0.69  0.72  0.71  0.72  0.68  0.66  0.57  0.45  0.35
                                    0.43  0.56  0.64  0.70  0.73  0.71  0.72  0.70  0.68  0.60  0.48  0.38V
                                   -0.03 -0.02 -0.02 -0.01 -0.01  0.00  0.00 -0.02 -0.02 -0.03 -0.03 -0.03V
```

**Figure 4. Total prompt thermal power (%) versus time**

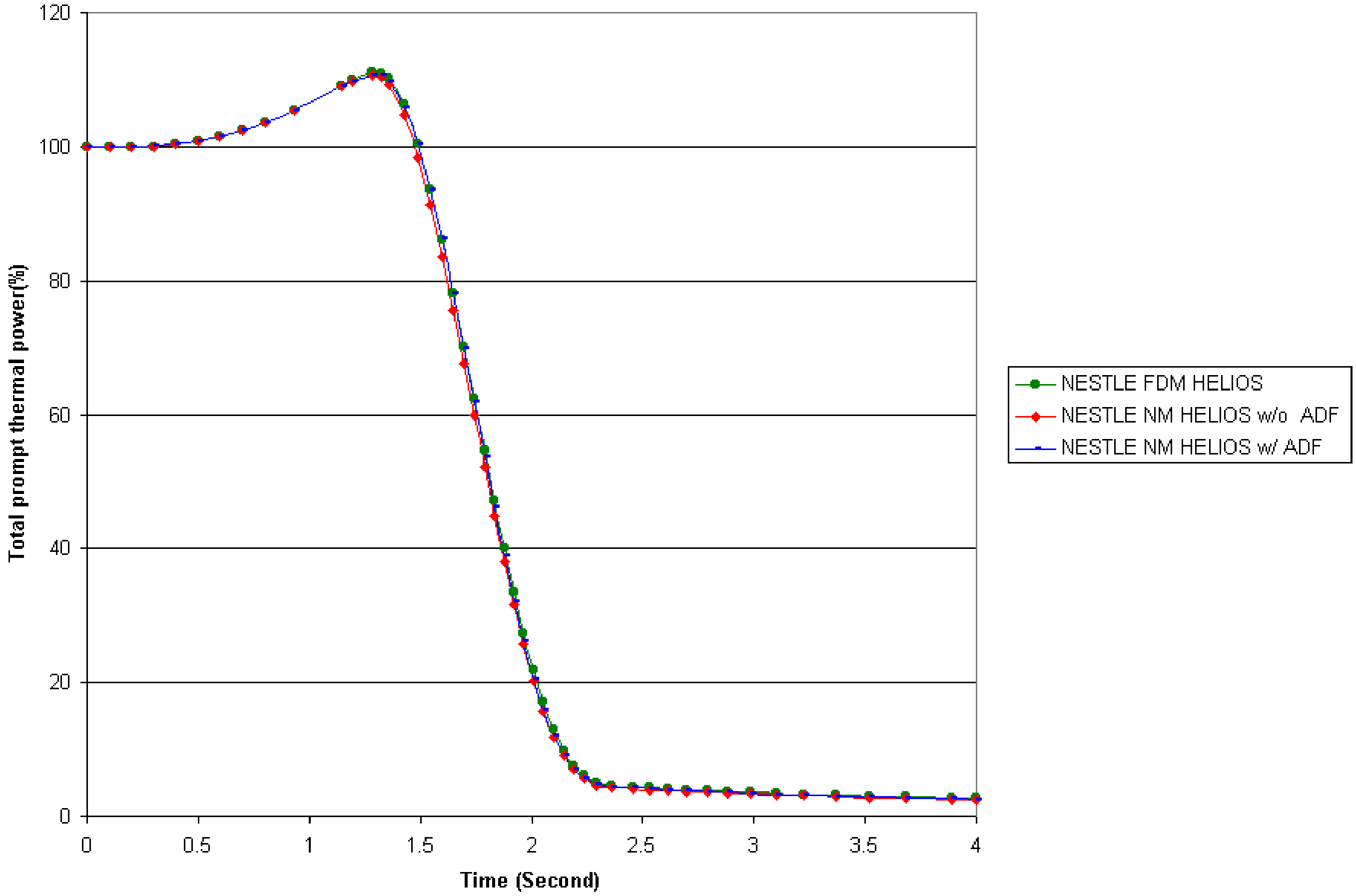

**Figure 5. Variation of total prompt thermal power as a function of time-step size refinement based upon NESTLE NM.**

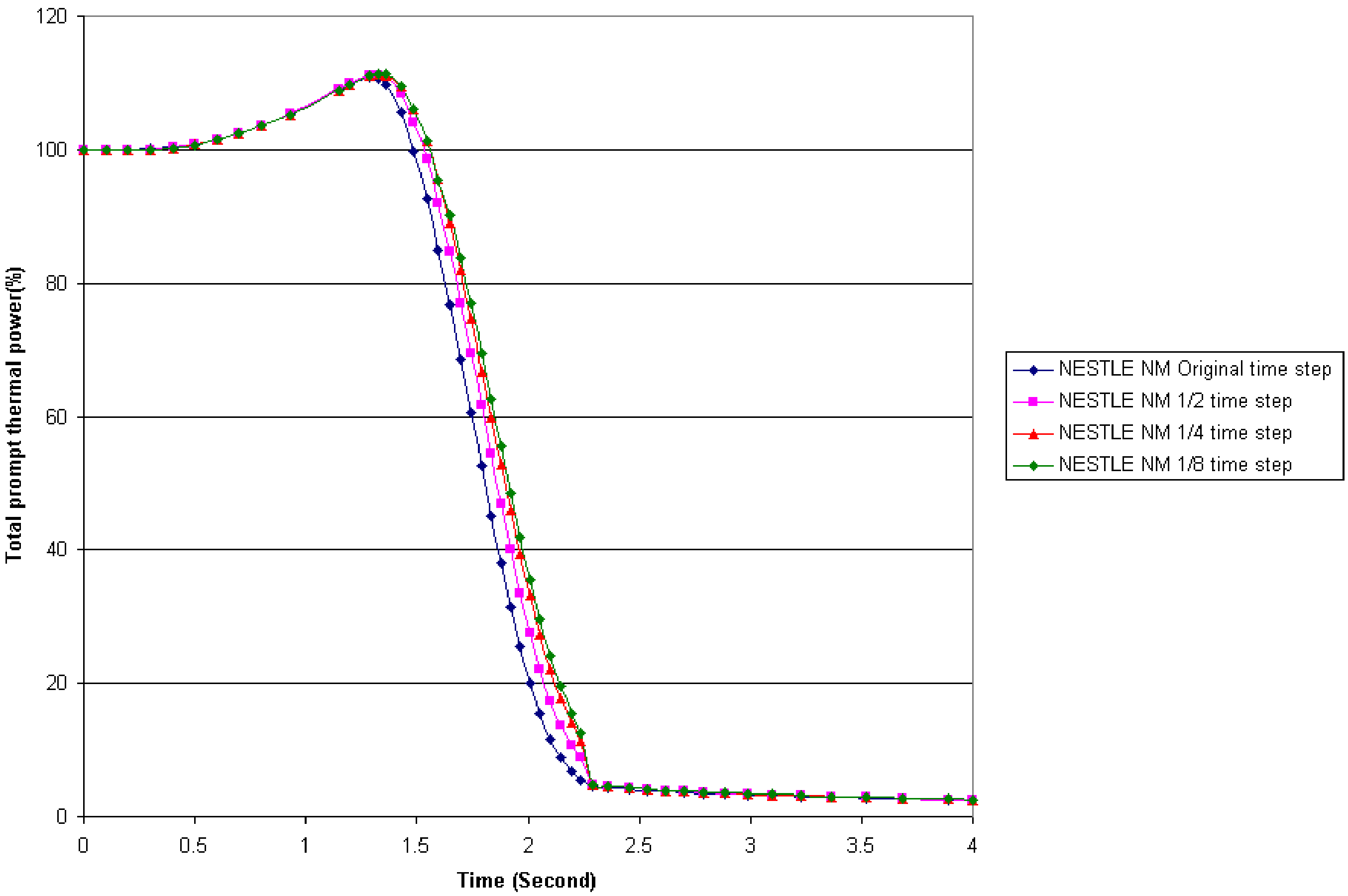

**Figure 6. Total prompt thermal power (%) versus time using HELIOS/DRAGON-H-based functionalized cross-sections with coolant density modified.**